ISSN: 2277-9655
Impact Factor: 5.164
CODEN: IJESS7

IJESRT
INTERNATIONAL JOURNAL OF ENGINEERING SCIENCES & RESEARCH TECHNOLOGY

INVESTIGATION OF EFFECT OF MECHANICAL PROPERTIES OF DIFFERENT SHAPED NOTCHED AROUND THE SPECIMEN UNDER FRICTION STIR HOLE EXPANSION

Vishwanath K.C [*1], Dr. Thirtha Prasada H.P [2]
[*1] Research Scholar, VTU-RRC,Belgaum. Assistant professor, Department of Mechanical Engineering, RajaRajeswari College of Engineering, Bangalore, Karnataka,India.
[2]Associate Professor, VTU-CPGS, Muddhenahalli, Chikkaballapur(D), Karnataka,India.

DOI: 10.5281/zenodo.1345627

ABSTRACT
The aim of the research work was to investigate on the effect of experimental testing on the test specimens for cast, cold hole expansion and stir hole expansion conditions. For as cast condition, the specimens with different K_t values were designed by referring to a data hand book. The specimens with different notch radii were then fabricated from a larger sheet of Aluminium 6061 by wire cutting method. The wire cut method was used as it gave a very accurate dimensional tolerance. A Universal Testing Machine (UTM) was used to perform tensile testing of the fabricated specimens. The notched specimens were subjected to tensile loading. Loading was applied incrementally to local strain measurements being made at each interval with the help of strain gauge, attached at the vicinity of the notch.

KEYWORDS: Aluminium alloys, Friction stir drilling, UTM, FSHE.

I. INTRODUCTION
Many work focused to develop the aircraft structure based on combined loading situation for critical operating conditions. Generally aircraft-components always subjected to fatigue and dynamic loading condition and failure is very difficult to detect / predict. Along with poor effective design of highly complex aircraft members they are engine exhaust system, airframe and other structural members which are contribute premature failure of the components. High fatigue loads which leads to acoustics and decrease the fatigue life of the structure. Hence aerospace structure needs a multidisciplinary computational analysis to analysis their integrity for future aircraft designs. Modern aerospace research and technology is continuously developing novel technology to fulfill the global demand for requirement of aircrafts. It needs major improvement to change intervals of flight, rapid protection and safety defense mechanism in the aircraft industries. During critical flight operation many components such as aircraft outer Skelton which embedded with gas turbine exhaust system failed prematurely due to nonlinear operating conditions and extreme environmental condition such as higher temperature, intensive acoustic effect and unbalanced structural loads applied during the flight of aircraft.

The market for fastener holes looks very promising. Safety being the uttermost concern in aircraft industry, any failure of fastener holes is non-negotiable. That is the reason why, analyst predicts the market worth of fastener holes will rise from USD 5.49 Billion in 2016 to USD 7.73 Billion in 2021. It is not just aircraft industry; fasteners are widely used in automobile industry as well as for manufacture of furniture and electronic appliances. One of the most important industries for the fastener is the automotive industry. With ever increasing demand of SUVs and Sedans, the market growth of fasteners is inevitable. Furthermore, the increased demand of lifts in malls and offices is going to propel the market for fasteners. Even the advancement in the field of medical such as CT scanner and ECG machines can prove to be beneficial to fastener market. However, recent developments in the field of ducts and tapes are the only hindrances to the growth of market for fasteners.

To exploit its potential in aero-engine industry, where operating stresses are very high due to weight considerations, one needs to understand the influence of compressive strain applied through the cold-expansion mandrel on the residual stress field, influence of external load parameters such as the frequency of load application, major-minor fatigue cycle interaction, operating temperature and associated fatigue/creep interaction.

ISSN: 2277-9655
Impact Factor: 5.164
CODEN: IJESS7

II. MATERIALS AND METHODS

The detailed experimental testing was performed on the test specimens for as cast, cold hole expansion and stir hole expansion conditions. For as cast condition, the specimens with different K_t values were designed by referring to a standard publication. The specimens with different notch radii were then fabricated from a larger sheet of Aluminium 6061 by wire cutting method. The wire cut method was used as it gave a very accurate dimensional tolerance. A Universal Testing Machine (UTM) was used to perform tensile testing of the fabricated specimens.

2.1 Tensile elastoplastic behaviour :

2.1.1 Specimen Design:

In this section, specimen design has been discussed. Aluminium alloys are promising materials in aerospace, medical and sports applications because of their unique properties, and in particular the relatively large deformations and recovery forces that can be achieved. Hence aluminum 6061-T6 alloy was considered as the specimen material.

2.1.2 Specimen Design Calculations

Specimen design calculations were calculated taking into account some important parameters as shown in Fig. 1.

- The dimensions of the specimen were adopted from the work carried out by Z Zeng et.
- The thickness of the specimen was calculated so as to prevent buckling using the relation,

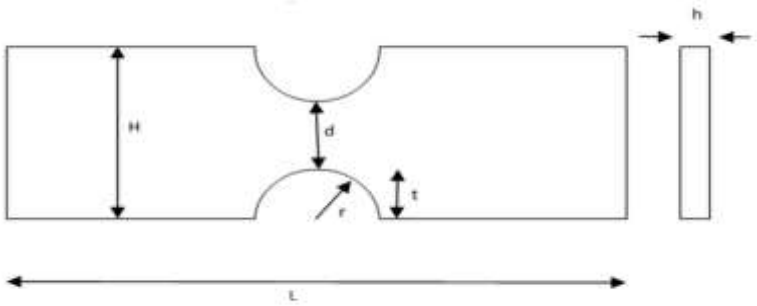

$$\sigma_u = \frac{4\pi^2 Eh^2}{12L^2}$$

Where, σ_u : Ultimate tensile Strength

E : Modulus of Elasticity
h : Thickness of the specimen
L : Gauge length of the specimen
For the given specimen,

Ultimate Tensile strength σ_u = 310 MPa
Length L= 60.32 mm
Young's Modulus E= 69 GPa

$$310 = \frac{4\pi^2 \left(69\times10^3\right)\times h^2}{12\times60.32^2}$$

$\therefore$ h= 4.3 mm

As the standard thickness of the aluminium 6061 alloy available in the market is 4 mm, the aluminium alloy sheet of 4 mm thickness was selected. The stress concentration factor K_t of the specimen is calculated using the relation given in the following Table1 taken from Metallic materials properties development and standardization (MMPDS) Data Hand Book[17].

2.1.3 CAD models of the specimen

The CAD models of the specimen for different Kt values were created using CATIA V5 software. Fig. 2(a), (b), (c) and (d) show CAD models of the specimen for stress concentration factors ranging from 1.75, to 4.5. Table 1 shows the plate with notch radius of 9.23mm, plate thickness of 4mm, gauge length 60.32mm, and width of 41.28mm.

Table 1 Specimen Dimensions for Kt=1.75

ISSN: 2277-9655
Impact Factor: 5.164
CODEN: IJESS7

Parameter	Dimension (in mm)			
	K_t values			
	1.75	**2.0**	**4.25**	**4.50**
Notch Radius	9.23	7.10	5.25	3.50
Plate Thickness	4.00	4.00	4.00	4.00
Gauge Length	60.32	60.32	60.32	60.32
Width	41.28	41.28	41.28	41.28
Fillet Radius	11.11	11.11	11.11	11.11

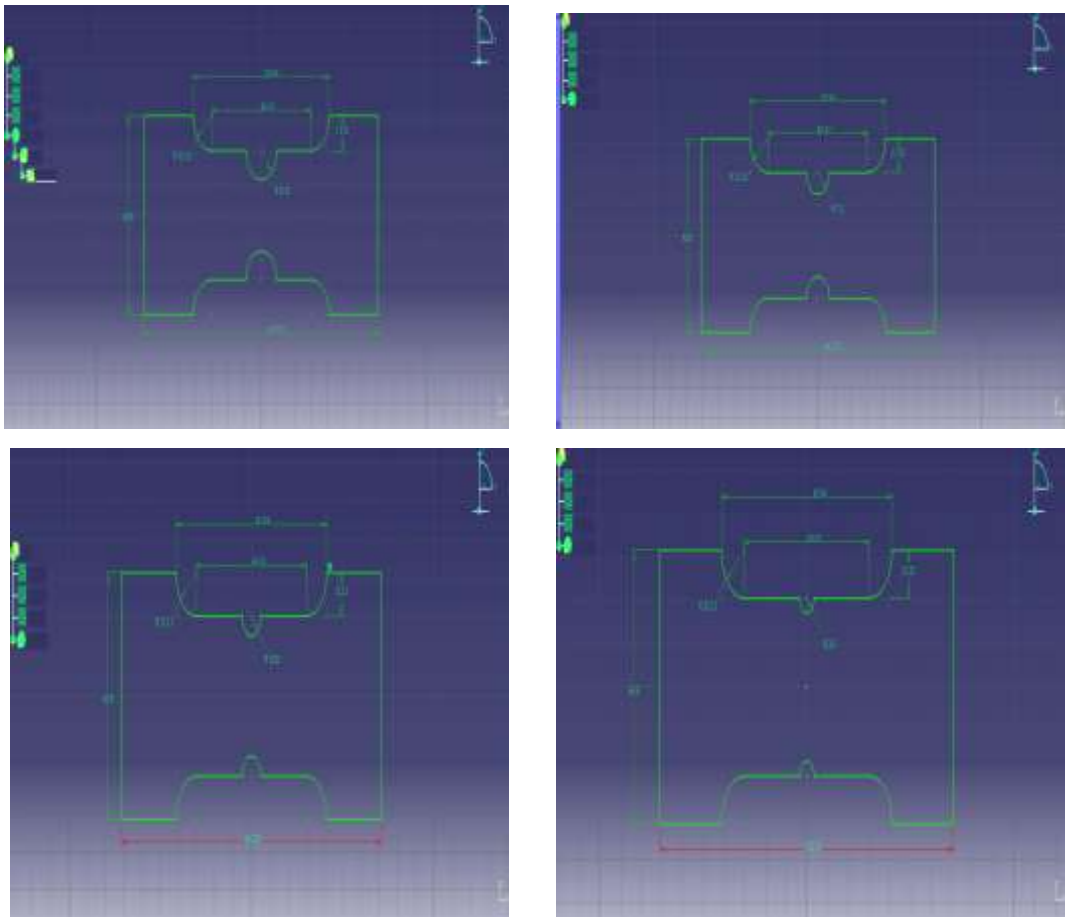

Fig. 2 Geometrical drawing of the specimens for different K_t values a) 1.75, b) 2.0, c) 4.25 and d) 4.50

ISSN: 2277-9655
Impact Factor: 5.164
CODEN: IJESS7

2.1.4 Fabrication of test specimen

The test specimen was designed by referring the standard papers . Suitable calculations were made to make sure buckling did not occur under compression. Four different specimen designs with different stress concentration factors were conceived and eight specimen of each design were fabricated. Wire cutting method was used to cut the specimens from the aluminium alloy sheet. The Fig. 3 below shows the wire cutting apparatus used for wire cutting of the specimens.

Fig. 3 Specimens after FSHE

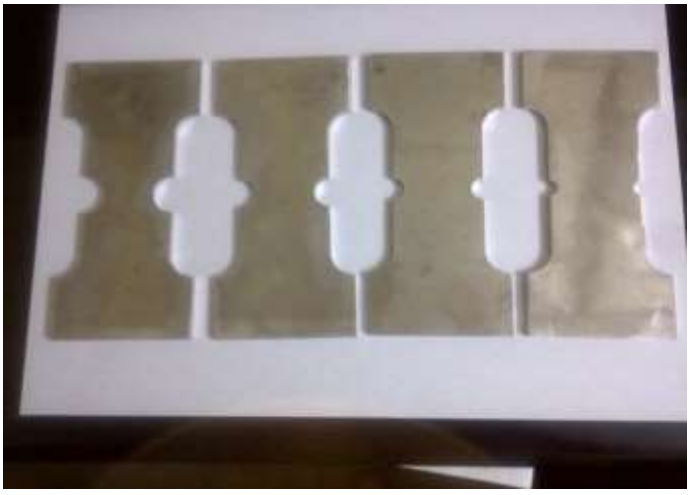

Fig. 4 Below shows the specimens fabricated by the wire cutting method.

III. RESULTS AND DISCUSSION

Tensile tests were performed on the specimens using a computerized Universal Testing Machine (UTM). The machine used was UTE-10. The specifications of the machine are shown in the Table 2.

ISSN: 2277-9655
Impact Factor: 5.164
CODEN: IJESS7

Table 2 UTM specification used for testing

Model/ Type	UTE 10
Machine Make	FINE SPAVY
Capacity	100 KN
Force Indicator Make	FASNE
Uncertainity of measurement	The reported uncertainity is at coverage factor k=2 which corresponds to a coverage probability of approximately 95.45% for a normal distribution.

The experimental setup used for the conduction of tensile test is shown below in Fig. 5.

Fig. 5 Computerised Universal Testing Machine

3.1 Specimen Setup

As the specimen (Aluminuim 6061) had a smooth surface, it had to be roughened at the ends, so that it could be held in the grippers effectively without slipping. A strain gauge was mounted on the specimen at the vicinity of the notch root, as the mounting of the strain gauge exactly at the notch root was difficult, owing to very small width of the plate and curvature of the notch. The strain gauge was mounted on the specimen at the point shown in the Fig. 6(a) and 6(b)

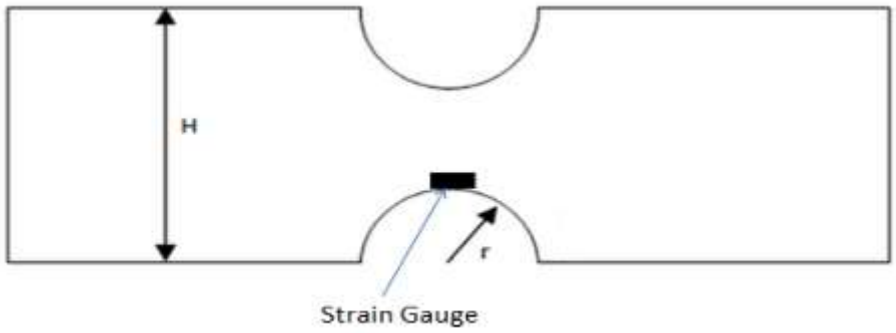

Fig. 6(a) Positioning of strain gauge

ISSN: 2277-9655
Impact Factor: 5.164
CODEN: IJESS7

Fig. 6 (b) Positioning of strain gauge

Table 3 Specification of strain gauge

Gage Type	Foil type.
Nominal Resistance	350 Ohms +/-0.1%
Gage Factor	4.10 +/-1%
Grid Size L & W	3.0 X 3.1mm
Overall Size L & W	7.2 X 4.9mm
Voltage	5 V to 15 VDC
Hysteresis	+/- 0.1% of R.O
Zero balance compensated	+/- 2%
Temperature Range	-5 Deg C to 65 Deg C
Termination	With Leads
Maximum Strain	20,000 Micro strains

The strain gauge was then wired to the microstrain indicator which gave the direct reading of the strain. The Fig. 7 below shows the strain indicator and the load indicator setup.

3.2 Specimen Loading

The specimen was then fixed on the UTM. The UTM loading was done gradually via the computer software. As the load was being applied, the microstrain readings were noted down corresponding to the respective loads, from the strain indicator. The maximum load applied was 26.4kN. The Fig. 8 below shows the specimen fixed on the UTM machine.

The experiment was repeated for the specimens with different stress concentration factors and the values of loads and the corresponding strains were recorded. The load and the strain values obtained from the tensile testing of the specimen with Kt=4.5 (radius=3.5 mm) is tabulated below in Table 4.

Fig. 7 Strain gauge synced with UTM

ISSN: 2277-9655
Impact Factor: 5.164
CODEN: IJESS7

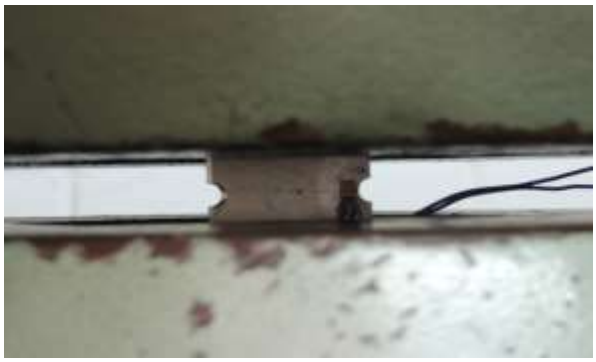

Fig. 8 Specimen fixed on UTM

Table 4 Tensile Testing Data for Kt=4.5

Load (kN)	Obtained strain (microstrains)
4.64	700
5.28	1360
7.92	1819
10.56	2526
13.2	3782
15.84	4946
18.48	6729
21.12	7823
23.76	9468
26.4	9919

3.3 Determination of Strain at Notch root

As the strain gauges were mounted at the vicinity of the notch and not at the notch root, it was essential to determine the strains at the notch root. This was done by using the strain values from the numerical analysis at the notch root and also at the point where strain gauge was mounted. The Fig. 9 below shows the arrangement of the strain gauge on the specimen and the points at which the strain from the strain gauge is obtained.

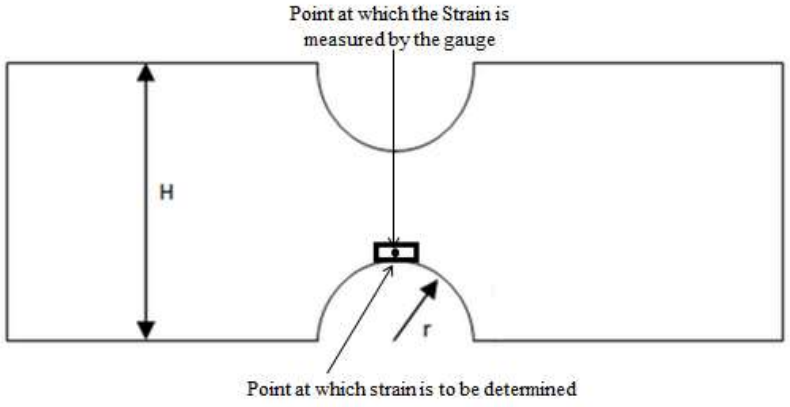

Fig. 9 Strain gauge mounting

ISSN: 2277-9655
Impact Factor: 5.164
CODEN: IJESS7

Let Xa= the strain obtained from ANSYS at the center of the strain gauge.
Ya= the strain obtained from ANSYS at the notch root
Xe= the experimental strain obtained by the strain gauge
Ye= the experimental strain to be determined at the notch root.
Assuming that the ratios of the strains at the two points is same in numerical analysis and in experiment, we get the following relation,

$$\frac{Y_e}{X_e} = \frac{Y_a}{X_a}$$

Thus we get,

$$Y_e = \frac{Y_a}{X_a} \times X_e$$

From the above relation equaiton we get the experimental strain at the notch root.

3.4 Sample calculation of Experimental strain at the notch root:
For the specimen with Kt=4.5 (radius=3.5 mm),
At load step 1,
Load= 2640 N
Strain obtained from ANSYS at the center of the Strain gauge, Xa=0.000444
Strain obtained from ANSYS at the notch root, Ya=0.00114
Experimental strain obtained by the strain gauge Xe=.0007

Hence,

$$Y_e = \frac{Y_a}{X_a} \times X_e$$

$$\therefore Y_e = 0.001793$$

IV. CONCLUSION

The experiment was conducted to measure the cold hole expansion and stir hole expansion conditions. CAD models of the specimen for stress concentration factors ranging from 1.75, to 4.5, it shows the plate with notch radius of 9.23mm, plate thickness of 4mm, gauge length 60.32mm, and width of 41.28mm. A strain gauge was mounted on the specimen at the vicinity of the notch root, as the mounting of the strain gauge exactly at the notch root was difficult, owing to very small width of the plate and curvature of the notch. The UTM loading was done gradually via the computer software. As the load was being applied, the microstrain readings were noted down corresponding to the respective loads, from the strain indicator. The cold hole expansion was done for Al 6061 alloy based on their strength, high specific strength, resistance and corrosion.

V. ACKNOWLEDGEMENTS

This research was supported/partially supported by Research Center VTU-RRC, Belgaum and RajaRajeswari college of Engineering, Bangalore. We thank to Dr. N. Chikkanna, Professor, VTU-PG center, Muddhenahalli, Chickballapur (D), and Dr. Hemalatha K.L, Professor, SKIT, Bangalore. Who provided insight and expertise that greatly assisted the research, although they may not agree with all of the interpretations of this paper. My sincere thanks to Dr. Thirtha Prasada H.P Associate, Professor. Dept. of CAE, VTU-PG center, Muddhenahalli, Chickballapur (D), for their support and cooperation during the preparation of this Research Article.

VI. REFERENCES

1. Hardrath HF and Ohman H, A study of elastic plastic stress concentration factors due to notches and fillets in flat plate, NACA Technical, Report 2566; 1951.
2. Gemma E. An approximate elasto-plastic analysis of the effect of plane strain at the surface of a notch, Engineering Fracture Mechanics, 1985, 22(3), 495–501.
3. Hoffmann M and Seeger T., A generalized method for estimating multiaxial elastic–plastic notch stresses and strains, Part 1- Theory, Journal of Engineering Materials and Technology, 1985, 107(4), 250–254.
4. Z Zeng, Elasto-plastic stress and strain behavior at notch roots under monotonic and cyclic loadings, Journal of Strain Analysis, 36(3), 2001, 287-300.
5. G.V. Dunchev, J. T. Maximov and N. Ganev, A new conception for enhancement of fatigue life of large number of fastener holes in aircraft structures, Fatigue and Fracture of Engineering, Materials and Structures, 2016.
6. Azushima, A., Koop, R., Korhonen, A., Yang, D.Y., Micari, F., Lahoti, G.D., Groche, P., Yanagimoto, J., Tsuji, N., Rosochowski, A. and Yanadida, A, Severe plastic deformation (SPD) process for metals, CIRP Annals – Manufacturing Technology, 57, 716–735.
7. Valiev, R.Z., Islamgaliev, R.K. and Alexandrov, I.V., Bulk Nanostructured materials from severe plastic deformation, Progress in Materials Science, 45, 103–189.
8. Shamdani, A.H. and Khoddam, S., A comparative numerical, study of combined cold expansion and local torsion of fastener holes, Fatigue Fracture Engineering Material Structure, 35,918–928.
9. Christ, R.J., Nardiello, J.A., Papazian, J.M. and Madsen, J.S. Device and method for sequentially cold working and reaming a hole, USA Patent 7770276.
10. Panaskar, N. J. and Sharma A Surface modification an nanocomposite layering of fastener hole through friction stir *processing*, Material Manufacturing Processes, 29, 2014,726–732.

CITE AN ARTICLE

Vishwanath, K. C., & Thirtha Prasada, H. P., Dr. (2018). INVESTIGATION OF EFFECT OF MECHANICAL PROPERTIES OF DIFFERENT SHAPED NOTCHED AROUND THE SPECIMEN UNDER FRICTION STIR HOLE EXPANSION. *INTERNATIONAL JOURNAL OF ENGINEERING SCIENCES & RESEARCH TECHNOLOGY*, *7*(8), 324-332.